

Fano enhancement of SERS signal without increasing the hot spot intensity

Selen Postaci^{1,2,*}, Bilge Can Yildiz³, Alpan Bek^{2,4,5}, and Mehmet Emre Tasgin¹

¹*Institute of Nuclear Sciences, Hacettepe University, 06800, Ankara, Turkey*

²*Department of Physics, Middle East Technical University, 06800, Ankara, Turkey*

³*Department of Applied Physics, Atilim University, 06836, Ankara, Turkey*

⁴*The Center for Solar Energy Research and Applications (GUNAM),*

Middle East Technical University, 06800, Ankara, Turkey

⁵*Micro and Nanotechnology Program of Graduate School of Natural and Applied Sciences,*

Middle East Technical University, 06800, Ankara, Turkey

(Dated: May 22, 2018)

Plasmonic nanostructures enhance nonlinear response, such as surface enhanced Raman scattering (SERS), by localizing the incident field into hot spots. The localized hot spot field can be enhanced even further when linear Fano resonances (FR) take place in a double resonance scheme. However, hot spot enhancement is limited with the modification of the vibrational modes, the break-down of the molecule and the tunnelling regime. Here, we present a method which can circumvent these limitations. Our analytical model and solutions of 3D Maxwell equations show that: enhancement due to the localized field can be multiplied by a factor of 10^2 to 10^3 . Moreover, this can be performed without increasing the hot spot intensity which also avoids the modification of the Raman modes. Unlike linear Fano resonances, we create a path interference in the nonlinear response. We demonstrate on a single equation that enhancement takes place due to cancellation of the contributing terms in the denominator of the SERS response.

I. INTRODUCTION

Metal nanoparticles (MNPs) confine incident electromagnetic field into nm-size hot spots as plasmonic oscillations. Field intensity at the hot spots can be 5 orders of magnitude larger compared to the incident one^{1,2}. It is also reported that self-repeating cascaded materials can confine light even better compared to the gaps between MNPs^{3,4}. Intense fields give rise to appearance of nonlinear processes such as second harmonic generation (SHG), four wave mixing (FWM), and surface enhanced Raman scattering (SERS)⁵⁻⁷. Actually, enhancement is squared since the field of the converted frequency is also localized⁸. In an efficient conversion, nonlinear process takes place between plasmonic excitations of different frequencies due to the localization⁹⁻¹¹. Recent studies show that MNPs with plasmon resonances at both excitation and Stokes frequencies (double resonance) provide better enhancement factors for Raman intensities¹¹⁻¹³.

Hot spots also provide enhanced light-matter interaction. When a quantum emitter (QE) is placed into a hot spot, localized plasmon field interacts strongly with the QE. Small decay rate of the QE creates Fano resonances, a dip in the plasmonic spectrum^{14,15}. In this process, the localized plasmon field provides the weak hybridization. Fano resonance also appears when excited plasmon mode couples to a long-live dark plasmon mode¹⁴⁻¹⁷.

Fano resonances can extend the lifetime of plasmon excitations¹⁸⁻²¹ which makes the operation of coherent plasmon emission (spaser) possible²². They also lead to further enhancement of the localized hot spot field²³. This extra enhancement in the hot spot field is cleverly adopted for the enhancement of the nonlinear response in FWM²⁴ and SERS^{4,25,26}. Similar to double resonance scheme¹¹, both the excited and Stokes shifted frequencies

are aligned with two Fano resonances^{4,25,26}. The double Fano resonance scheme provides much stronger enhancement in the SERS signal. Fano resonances are also shown to provide control over other nonlinear processes such as SHG^{27,28}, third harmonic generation²⁹, and FWM^{30,31}.

SERS is a very useful imaging technique. It provides information about the chemical composition of newly synthesized molecules by determining the existing bond types. Single-molecule detection via SERS is studied in many fields of science, including chemistry³², nanobiology³³, tumor targeting and cancer applications³⁴. Even more, mapping of inner structure and surface configuration of a single molecule is achieved recently³² using a double resonance scheme¹¹. Such an imaging requires very intense fields at the nm-size hot spots. When the imaging tip gets closer to the metal surface, the intensity at the hot spot –where the molecule lies– increases. If the hot spot intensity is increased further, e.g. via a double Fano resonance scheme^{4,25,26}, fragile molecules can be damaged^{35,36}. It is also experimented that vibrational modes of a Raman-imaged nanostructure (i.e. a carbon nanotube) can be modified due to the close spacing of the tip³⁷. Additionally, electron tunnelling can limit the intensity enhancement in the gaps³⁸.

In this manuscript, we study the SERS signal from a double resonance system. A Raman reporter molecule is placed close to the gap of a MNP dimer, see Fig. 1. We additionally place an auxiliary QE (e.g. a molecule or a nitrogen vacancy centre) to the other side of the gap. 3D solutions of Maxwell equations show that SERS can be enhanced by a factor of 10^3 without increasing the field intensities at the excited and the Stokes-shifted hot spots. This enhancement multiplies the enhancement due to localization. On a basic analytical model, we demonstrate the underlying reason for the enhancement. Cou-

pling of the auxiliary QE with the Stokes-shifted plasmon mode modifies frequency conversion paths dramatically. It yields a cancellation in the denominator of the SERS response, i.e. Eq. (12). 3D simulations show that enhancement predicted by the analytical model, also appears in the presence of retardation effects.

The presented phenomenon can be adopted to further increase the efficiency of SERS imaging for systems which are already operating in the break-down or tunnelling regimes. Better signal intensities with larger tip-surface spacing or with smaller laser intensities can be achieved by avoiding modifications in the Raman vibrational modes.

Our problem setting, which involves configuration of a MNP dimer coupled to a Raman reporter molecule and an auxiliary QE, can be implemented controllably using several nanotechnological methods such as e-beam lithography^{39,40} or DNA based biomolecular recognition^{41,42} that provide ultimate nanoscale spatial control⁴³. One can also conduct an experiment based on the stochastic distributions of many molecules²⁷. A practical implementation would be the following. A gold coated AFM tip decorated (can also be considered as contamination) with carefully chosen auxiliary molecules (QEs) as shown in Fig. 2, using a technique reminiscent of dip-pen lithography, will produce more intense SERS signal without increasing near-field intensity. In spasers²², where MNPs are surrounded by molecules, linear Fano resonance increases the plasmon lifetime and fluorescence intensity of the molecules³. Fano resonances can also be adopted in an all-plasmonic setting^{44,45}.

In the following, we first present the basic analytical model from which we anticipate the presence of the enhancement. We introduce the effective Hamiltonian for a double resonance SERS system coupled with an auxiliary QE. We obtain the equations of motion (EOM) using Heisenberg equations. We manage to obtain a simple expression for the steady-state of the Stokes field amplitude, Eq. (12). On this expression we explain why such an enhancement should emerge. Next, we perform simulations of the exact solutions of the 3D Maxwell equations in order to test the retardation effects. In this case, the spectrum for which enhancement appears narrows down compared to the analytical result. Even so, an enhancement of 3 orders of magnitude on top of the localization can be observed.

II. HAMILTONIAN AND EQUATION OF MOTION

We consider a double resonance scheme with two plasmon bands, \hat{a} and \hat{a}_R , with resonances $\Lambda = c/\Omega=532$ nm and $\Lambda_R = c/\Omega_R=780$ nm respectively, see Fig. 1. A strong incident laser field, $\lambda_L = c/\omega=593$ nm, excites the plasmon polaritons in the \hat{a} -mode. The substantial overlap between the hot spots of the two modes, \hat{a} and \hat{a}_R , and the Raman reporter molecule yields a signifi-

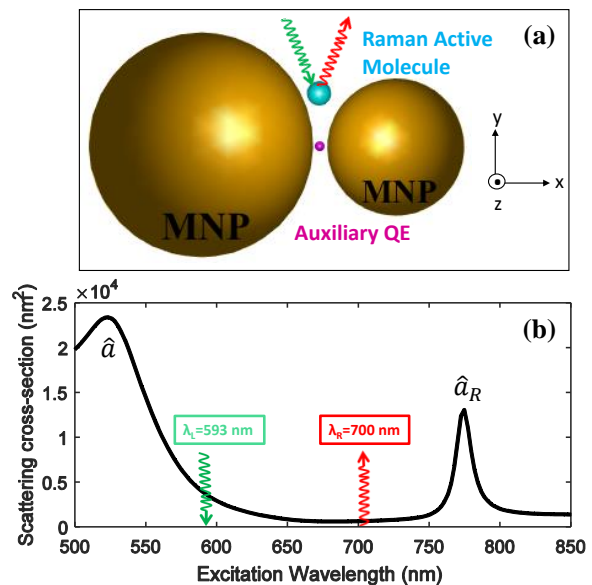


FIG. 1. (a) The setup we use in the 3D solutions of Maxwell equations. A gold MNP dimer, of radii 90 nm and 55 nm, creates a hot spot in the 4 nm gap. A sphere of 4 nm radius (blue), representing a Raman reporter, is placed close to the hot spot for producing the SERS signal. We place an auxiliary QE (purple) also at the hot spot of the dimer, for enhanced interaction with the \hat{a}_R plasmon mode. We move it along the z-direction when we desire to decrease the plasmon-auxiliary QE coupling, f . (b) Linear response of the dimer shows two plasmon peaks at $\Lambda=530$ nm and $\Lambda_R=780$ nm. System is excited by a $\lambda_L=593$ nm laser and a Stokes shifted signal emerges at $\lambda_R=700$ nm. λ_L and λ_R overlap with Λ and Λ_R , respectively. The λ_{eg} of the molecule is chosen to couple with the \hat{a}_R -mode, see Fig. 3a. We use parameters similar to (b) in producing an accompanying simulation within our simple model Eq. (1). Experimental data of gold (dimer) and a Lorentzian dielectric function (auxiliary QE), in MNPBEM⁴⁶, are used for the 3D simulations.

cant overlap integral χ for the Stokes Raman process. Hence, a plasmon in the excited \hat{a} mode generates a Stokes shifted plasmon polariton with $c/\omega_R = \lambda_R=700$ nm in the lower energy mode \hat{a}_R ¹¹⁻¹³.

When an auxiliary QE is inserted in the system, it also interacts strongly with the hot spot of \hat{a}_R -mode, into which the nonlinear conversion takes place. Level spacing of the QE, ω_{eg} , is chosen about Ω_R .

Hamiltonian for such a system, including the Raman conversion, can be written as the sum of the terms $\hat{H}_0 + \hat{H}_{QE} + \hat{H}_L + \hat{H}_{int} + \hat{H}_R$, with

$$\begin{aligned}
 \hat{H}_0 &= \hbar\Omega\hat{a}^\dagger\hat{a} + \hbar\Omega_R\hat{a}_R^\dagger\hat{a}_R + \hbar\Omega_{ph}\hat{a}_{ph}^\dagger\hat{a}_{ph} \\
 \hat{H}_{QE} &= \hbar\omega_{eg}|e\rangle\langle e| \\
 \hat{H}_L &= i\hbar(\hat{a}^\dagger\epsilon e^{-i\omega t} - \hat{a}\epsilon^* e^{i\omega t}), \\
 \hat{H}_{int} &= \hbar(f\hat{a}_R|e\rangle\langle g| + f^*\hat{a}_R^\dagger|g\rangle\langle e|), \\
 \hat{H}_R &= \hbar\chi(\hat{a}_R^\dagger\hat{a}_{ph}^\dagger\hat{a} + \hat{a}^\dagger\hat{a}_{ph}\hat{a}_R),
 \end{aligned} \tag{1}$$

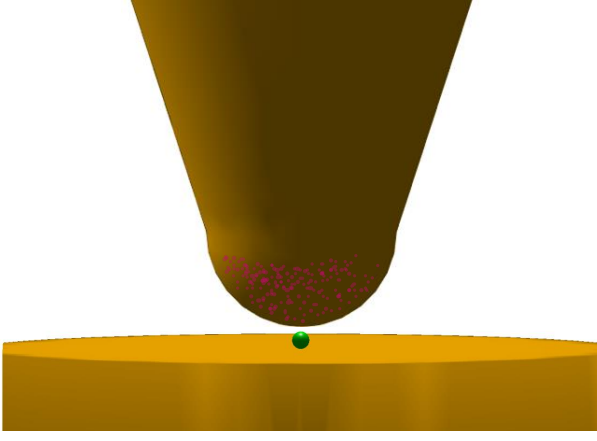


FIG. 2. A practical implementation of the extra enhancement. A gold coated AFM tip is decorated (can as well be named as contamination) by the auxiliary QEs (purple). The auxiliary QEs, with a level spacing not close to either the exciting or the SERS frequency, do not cause an alteration of the hot-spot field intensity at the location of the Raman reporter molecule (blue), yet they give rise to further enhancement of the SERS from reporter molecule due to Fano effect.

where \hat{H}_0 includes the energies for the driven \hat{a} , and Raman shifted \hat{a}_R plasmon modes as well as the molecular vibrations, \hat{a}_{ph} . \hat{H}_{QE} is the energy of the auxiliary QE. \hat{H}_L is the laser pump, \hat{H}_R denotes the Raman process and \hat{H}_{int} is the interaction of the Stokes-shifted plasmon polaritons of \hat{a}_R -mode with the auxiliary QE. χ determines the strength of the Raman process, while ε denotes the power of the incident laser source. Here, we do not consider the anti-Stokes shift in the Hamiltonian to simplify our results, however, we have verified that the enhancement values and the spectroscopic behaviour of the system remain similar in such a case. The interaction strength between the auxiliary QE and \hat{a}_R -mode is denoted by f . Coupling of the auxiliary QE to \hat{a} -mode is not considered due to far-off-resonance and simplicity. $|g\rangle$ and $|e\rangle$ represents the ground and excited states for the auxiliary QE. \hat{H}_R is a standard Hamiltonian for a Raman process, described, for instance, in the Refs.^{11–13}. A similar form of \hat{H}_R could have also been derived⁴³ from a radiation pressure like interaction^{47,48}. We obtain the dynamics via Heisenberg equations, $i\hbar\dot{\hat{a}} = [\hat{a}, \hat{H}]$. We note that, since we do not consider the quantum optical effects, we are able to replace the operators with complex numbers⁴⁹; $\hat{a} \rightarrow \alpha$, $\hat{a}_R \rightarrow \alpha_R$, $\hat{a}_{ph} \rightarrow \alpha_{ph}$, $\hat{\rho}_{eg} = |e\rangle\langle g| \rightarrow \rho_{eg}$. We find the EOM as

$$\dot{\alpha}_R = (-i\Omega_R - \gamma_R)\alpha_R - i\chi\alpha_{ph}^*\alpha - if^*\rho_{eg}, \quad (2)$$

$$\dot{\alpha} = (-i\Omega - \gamma)\alpha - i\chi\alpha_{ph}\alpha_R + \varepsilon e^{-i\omega t}, \quad (3)$$

$$\dot{\alpha}_{ph} = (-i\Omega_{ph} - \gamma_{ph})\alpha_{ph} - i\chi\alpha_R^*\alpha + \varepsilon_{ph}e^{-i\omega_{ph}t}, \quad (4)$$

$$\dot{\rho}_{eg} = (-i\omega_{eg} - \gamma_{eg})\rho_{eg} + if\alpha_R(\rho_{ee} - \rho_{gg}), \quad (5)$$

$$\dot{\rho}_{ee} = -\gamma_{ee}\rho_{ee} + if^*\alpha_R^*\rho_{eg} - if\alpha_R\rho_{eg}^*, \quad (6)$$

where we introduce the damping rates γ , γ_R , γ_{ph} , γ_{eg} ,

and γ_{ee} . We also have the constraint $\rho_{ee} + \rho_{gg} = 1$. ε_{ph} is introduced for the vibrations, due to the finite ambient temperature^{47,48}. Its actual value has no influence in the relative enhancement/suppression factors.

In the steady-state, solutions are in the form $\alpha_R(t) = \tilde{\alpha}_R e^{-i\omega_R t}$, $\alpha(t) = \tilde{\alpha} e^{-i\omega t}$, $\alpha_{ph}(t) = \tilde{\alpha}_{ph} e^{-i\omega_{ph} t}$, $\rho_{eg}(t) = \tilde{\rho}_{eg} e^{-i\omega_{eg} t}$, $\rho_{ee}(t) = \tilde{\rho}_{ee}$, where exponentials cancel in each equation, Eqs. (7)-(11). In other words, this is the energy conservation in the long term limit. Eqs. (2)-(6) become

$$[i(\Omega_R - \omega_R) + \gamma_R]\tilde{\alpha}_R = -i\chi\tilde{\alpha}_{ph}^*\tilde{\alpha} - if^*\tilde{\rho}_{eg}, \quad (7)$$

$$[i(\Omega - \omega) + \gamma]\tilde{\alpha} = -i\chi\tilde{\alpha}_{ph}\tilde{\alpha}_R + \varepsilon, \quad (8)$$

$$[i(\Omega_{ph} - \omega_{ph}) + \gamma_{ph}]\tilde{\alpha}_{ph} = -i\chi\tilde{\alpha}_R^*\tilde{\alpha} + \varepsilon_{ph}, \quad (9)$$

$$[i(\omega_{eg} - \omega_R) + \gamma_{eg}]\tilde{\rho}_{eg} = if\tilde{\alpha}_R(\tilde{\rho}_{ee} - \tilde{\rho}_{gg}), \quad (10)$$

$$\gamma_{ee}\tilde{\rho}_{ee} = -if\tilde{\alpha}_R\tilde{\rho}_{eg}^* + if^*\tilde{\alpha}_R^*\tilde{\rho}_{eg}. \quad (11)$$

We can obtain a simple expression for the Stokes-shifted plasmon amplitude (SERS signal) by using Eqs. (7) and (9)

$$\tilde{\alpha}_R = \frac{-i\chi\varepsilon_{ph}^*}{\beta_{ph}^* \left([i(\Omega_R - \omega_R) + \gamma_R] - \frac{|f|^2 y}{[i(\omega_{eg} - \omega_R) + \gamma_{eg}]} \right) - |\chi|^2 |\tilde{\alpha}|^2} \tilde{\alpha}, \quad (12)$$

where $\beta_{ph} = [i(\Omega_{ph} - \omega_{ph}) + \gamma_{ph}]$. Here $y = \rho_{ee} - \rho_{gg}$ is the population inversion for the auxiliary QE. $|\chi|^2 |\tilde{\alpha}|^2$ term is small compared to other ones in the denominator and hence, can be neglected.

We use Eq. (12) merely to anticipate the enhancement/suppression effects. All the presented results are obtained by numerical time evolution of Eqs. (2)-(6).

Enhancement. A quick examination of the denominator of Eq. (12) reveals that for the proper choice of ω_{eg} , nonresonant term $(\Omega_R - \omega_R)$ in the denominator can be cancelled with the term containing f , the MNP-QE coupling. This condition is

$$\omega_{eg}^* = \omega_R + \frac{|f|^2 y}{2(\Omega_R - \omega_R)} - \sqrt{\frac{|f|^4 |y|^2}{4(\Omega_R - \omega_R)^2} - \gamma_{eg}^2}. \quad (13)$$

This choice for the level spacing enables us to minimize the denominator, consequently enhancing the Raman signal amplitude. This type of enhancement does not necessitate an arrangement in the inner structure of plasmon modes.

To examine the dependence of the enhancement with respect to the level spacing ($\lambda_{eg} = c/\omega_{eg}$), we time evolve the EOM (2)-(6). The parameters are chosen as $\gamma = 0.01\omega$, $\gamma_R = 0.005\omega$, $\gamma_{ph} = 0.001\omega$. Nevertheless, one can realize that Ω_{ph} and γ_{ph} play no role in the cancellation of the denominator in Eq. (12). The damping rate (spectral width) of the auxiliary QE is taken to be $\gamma_{eg} = 10^{-5}\omega$. Here, the frequency of the incident light (ω) is related to λ_L as $\omega = c/\lambda_L = 593$ nm. χ is assumed a small value $10^{-5}\omega$, where it is verified that the value of χ does not affect the enhancement factors, and $\varepsilon = 0.1\omega$. f is also varied in order to explore the effect of the coupling in the MNP-QE system. The enhancement factor is calculated with respect to the $|\alpha_R|^2$ intensity for $f = 0$.

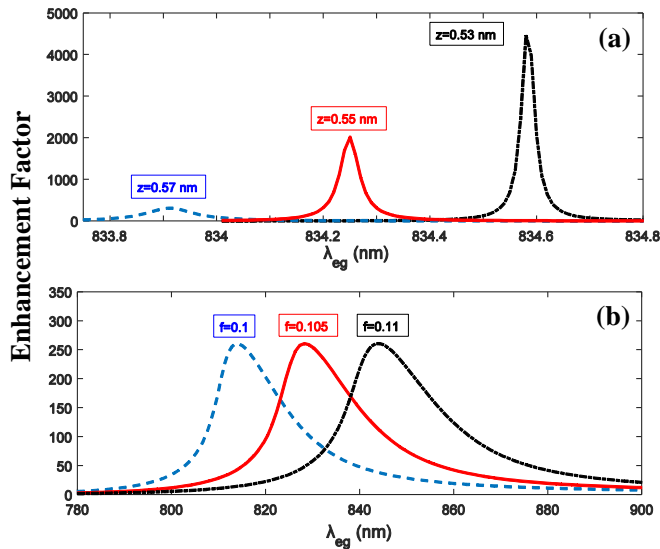


FIG. 3. Enhancement of the SERS signal with the presence of the auxiliary QE (purple) in Fig. 1. We plot the enhancement factors with respect to the level spacing ($\lambda_{eg} = c/\omega_{eg}$) of the auxiliary QE interacting with the \hat{a}_R plasmon mode, (Fig. 1b). Interaction of the auxiliary QE decreases with larger separations (z) to the hot spot. (a) Solutions of the 3D Maxwell equations for the system depicted in Fig. 1. Enhancement factors, multiplying localization effects, for SERS are calculated for three different positions of the auxiliary QE, $z=0.53$, 0.55 and 0.57 nm. At $z=0.0$ nm, we observe 2 orders of enhancement factor. The position of optimum $\lambda_{eg}^* = c/\omega_{eg}^*$, where maximum enhancement factor appears, shifts to larger wavelengths. Optimum $\lambda_{eg}^* \approx 834$ nm, is far away from the Stokes signal (700 nm). An enhancement due to a linear Fano resonance would yield maximum enhancement at $\lambda_{eg} \approx 700$ nm²³. Enhancement originates from the interference in the conversion paths as predicted by Eqs. (12)-(13). Intensities of both hot spots are unchanged. (b) Simulation of the enhancement factor using Eqs. (2)-(6) with the parameters similar to Fig. 1b. Simulations are for the presence of an auxiliary QE. We observe the similar behaviour in the position of optimum λ_{eg}^* , even though several complications involve in 3D simulations (a).

The results are depicted in Fig. 3(b), where enhancement factors of ≈ 300 are observed. As suggested by Eq. (13), $\Omega_R < \omega_R$, cancellation (enhancement) takes place for longer wavelengths as MNP-QE coupling, f , increases. The spectral position of $\lambda_{eg}^* = c/\omega_{eg}^*$ also justifies our assumption for off-resonant \hat{a} -QE coupling. If Eq. (12) is examined, it can be realized that the amount of enhancement can be increased by introducing more interference paths via additional QEs³⁰ or additional plasmon conversion modes.

Eq. (12) is a single and simple equation which enables us to predict possible interference effects without including the complications emerging in 3D simulations. Before moving forward, we underline that our aim is to present a simple understanding for the enhancement process, with-

out getting lost in details.

Linear Fano resonances, commonly referred in the literature, appear if one of the two coupled oscillators has longer lifetime^{14,16,17,50}. Here, interference of the nonlinear frequency conversion paths demonstrates us an interesting incident. Even when the spectral width (damping rate) of the auxiliary object is equal to the damping rate of the MNP hot spot, 25 times enhancement can emerge due to cancellation in the denominator of Eq. (12). The presented enhancement factor is obtained for a plasmon mode of fair quality $\gamma=0.01\omega$. When a higher quality MNP^{51,52} is used available enhancement factor grows up.

III. 3-DIMENSIONAL SIMULATIONS

We also perform simulations with the exact solutions of 3D Maxwell equations and use the setup in Fig. 1. We note in advance that we do not aim a one to one comparison between the analytical solutions and the 3D simulations. We aim to observe if the retardation effects wipe-out the enhancement phenomenon predicted by our basic analytical model. Making a one to one comparison between the theoretical findings and the 3D simulations, which is a very sophisticated process, is out of the scope of this work. In Fig. 1(a), we present a nano dimer with two gold spheres of radii 90 nm and 55 nm, whose linear response is depicted in Fig. 1(b). The dimer supports two plasmon modes at $\Lambda=c/\Omega=530$ nm and $\Lambda_R=c/\Omega_R=780$ nm. \hat{a} -mode is driven by a strong laser of wavelength $\lambda_L=593$ nm. We place a Raman reporter molecule with radius of 4 nm⁵³ (blue) close to the hot spot of the MNP dimer. For a “proof-of-principle” demonstration, we consider a single vibrational mode, $\nu = 2600$ cm⁻¹⁵⁴, for the Raman reporter molecule. The Stokes signal appears at $\lambda_R=700$ nm and couples to a_R mode of the double-resonance scheme¹¹. We model the auxiliary QE by a Lorentzian dielectric function $\epsilon(\omega)$ ² of resonance $\lambda_{eg} = c/\omega_{eg}$ and damping rate γ_{eg} . We compare the Raman intensities with the results where no auxiliary QE is present, i.e. enhancement factor.

In Fig. 3(a), we also change the position of the auxiliary QE along the z -axis in order to alter the interaction with the MNP. When distance to the hot spot centre (z), increases, the interaction of the plasmon mode with the auxiliary QE, [f in Fig. 3(b)] decreases. We observe that enhancement occurs at larger wavelengths for stronger MNP-QE coupling as suggested by the basic model. Furthermore, maximum enhancement in Raman signal takes place around $\lambda_{eg}^* \simeq 834$ nm, which is farther apart from the Stokes line $\lambda_R = 700$ nm. A linear Fano resonance would yield the strongest hot spot enhancement when $\lambda_{eg} \simeq \lambda_R$ ²³. λ_{eg}^* is in this regime both for our simple model and for 3D simulations. On the other hand, when auxiliary QE is positioned much closer to the dimer-centre, enhancement decreases 2 orders of magnitude⁴³. In this regime, excitations cannot be modelled with the presented treatment: strong hybridization

arises⁴³. This is also observed in SHG process²⁷. Even though many complications may arise in 3D solutions, e.g. coupling to dark modes in the MNP dimer, the results match “qualitatively” with our basic model as a “proof-of-principle” demonstration. Retardation effects allow Fano resonances to appear in a narrower band compared to our model, similar to Ref.¹⁰. We also note that our analytical model does not account for the change of density of states, i.e., Purcell factor.

It can be seen even in the simple setting of Fig. 1, a setting which can be optimized by further elaboration, an average of a factor of 10^2 to 10^3 further enhancement factor is achieved at a QE distance of ± 1 nm from the MNPs. It can be said that the hot spot field intensity within the 4 nm gap between MNPs is not a particularly strong one with respect to achievable hot spot enhancement factors of 10^5 - 10^6 at which an even larger distance between the QE and the MNPs could produce similar orders of further enhancement.

IV. SUPPRESSION

Our model also predicts that SERS can be suppressed several orders of magnitude, Fig. 4, for the choice of the auxiliary QE, $\omega_{eg} = \omega_R$. Simply, for this case, Fano resonance (transparency) prohibits the plasmon oscillations of the converted frequency ω_R from emerging into the \hat{a}_R -mode. One can realize that path interference in the nonlinear response is actually not so different from the one taking place in the linear response⁵⁰. That is, modification of the denominator both in the nonlinear^{10,30} and the linear response¹⁹ have a common form⁵⁵.

Similar silencing phenomenon is observed in the SHG experiments and in 3D simulations⁵⁶ and can be demonstrated with a simple analytical model¹⁰. Denominator of Eq. (12) also shows why a suppression effect can take place similar to the one observed in SHG⁵⁶. If one chooses $\omega_{eg} = \omega_R$, the extra term becomes $\gamma_{eg}^{-1}|f|^2y$. This term is very large since $\gamma_{eg}^{-1} \sim 10^5$ and $f=0.1$ in units scaled with the laser frequency ω (\approx PHz). We stress that Figs. 3(b) and 4 are generated through the exact time evolutions of Eqs. (2)-(6). That is, no approximation is used to obtain the results.

On the other hand, the suppression phenomenon – neither in the SHG¹⁰ nor in the Raman cases– cannot be demonstrated with the 3D simulations of Ref.⁵⁷. This is simply because 3D simulation method⁵⁷ is only a first-order approach. Demonstration of the suppression phenomenon necessitates the self-consistent solution of Maxwell equations, as in Eqs. (2)-(6). Self-consistent 3D simulation of a Raman process is a numerical art on its

own.

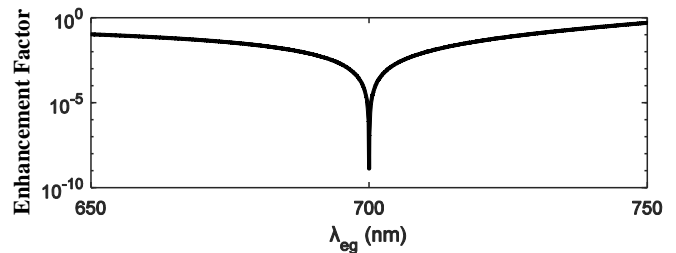


FIG. 4. Suppression of SERS for $\lambda_{eg} = \lambda_R$. When $\omega_{eg} = \omega_R$, $|f|^2y/\gamma_{eg}$ term in the denominator of Eq. (12) becomes very large, because γ_{eg} is very small compared to ω_R . This effect can be utilized to avoid losses due to Raman process in fiber laser applications.

V. SUMMARY AND DISCUSSIONS

We introduce a new method which can increase the SERS signal without increasing the hot spot intensities. In other words: SERS signal can be further multiplied by a factor of 10^2 - 10^3 , on top of the hot spot formation by plasmon mediated field enhancement, without heating the Raman reporter molecule further. This is different than linear Fano resonances which enhance the hot spot field^{4,25,26}. The phenomenon takes place due to the modification of the Raman conversion paths, in the presence of an auxiliary QE. Both the 10^2 - 10^3 enhancement and the unvarying hot spot intensities are confirmed with 3D simulations.

This phenomenon can be used not only to increase the Raman signal in materials already operating in the breakdown or tunnelling regimes and to avoid the modifications of vibrational modes. But it can also be adopted for high spatial resolution imaging of molecules. Raman signal emerges from the region where the two plasmon modes overlap spatially. When this overlap area is kept small, better spatial resolution can be obtained. However, SERS process also weakens with reduced overlap integral. The suggested method can help in increasing the SERS signal to observable values again.

The presented method is not physically intriguing only, but the model provides simple implementations, new phenomena and utilization of new enhancement tools.

ACKNOWLEDGMENTS

MET acknowledges support from TUBITAK Grant No: 1001-117F118 and TUBA-GEBIP 2017 support.

* saatciselen@gmail.com

¹ Mark I Stockman, “Nanoplasmonics: past, present, and glimpse into future,” *Optics express* **19**, 22029–22106

- (2011).
- ² Xiaohua Wu, Stephen K Gray, and Matthew Pelton, “Quantum-dot-induced transparency in a nanoscale plasmonic resonator,” *Optics express* **18**, 23633–23645 (2010).
 - ³ Christiane Höppener, Zachary J Lapin, Palash Bharadwaj, and Lukas Novotny, “Self-similar gold-nanoparticle antennas for a cascaded enhancement of the optical field,” *Physical review letters* **109**, 017402 (2012).
 - ⁴ Jinna He, Chunzhen Fan, Pei Ding, Shuangmei Zhu, and Erjun Liang, “Near-field engineering of fano resonances in a plasmonic assembly for maximizing cars enhancements,” *Scientific reports* **6**, 20777 (2016).
 - ⁵ Martti Kauranen and Anatoly V Zayats, “Nonlinear plasmonics,” *Nature Photonics* **6**, 737–748 (2012).
 - ⁶ Xia Hua, Dmitri V Voronine, Charles W Ballmann, Alexander M Sinyukov, Alexei V Sokolov, and Marlan O Scully, “Nature of surface-enhanced coherent raman scattering,” *Physical Review A* **89**, 043841 (2014).
 - ⁷ Li-Gang Wang, Sajid Qamar, Shi-Yao Zhu, and M Suhail Zubairy, “Manipulation of the raman process via incoherent pump, tunable intensity, and phase control,” *Physical Review A* **77**, 033833 (2008).
 - ⁸ Song-Yuan Ding, Jun Yi, Jian-Feng Li, Bin Ren, De-Yin Wu, Rajapandiyam Panneerselvam, and Zhong-Qun Tian, “Nanostructure-based plasmon-enhanced raman spectroscopy for surface analysis of materials,” *Nature Reviews Materials* **1**, 16021 (2016).
 - ⁹ Nicolai B Grosse, Jan Heckmann, and Ulrike Woggon, “Nonlinear plasmon-photon interaction resolved by k-space spectroscopy,” *Physical review letters* **108**, 136802 (2012).
 - ¹⁰ Deniz Turkpence, Gursoy B Akguc, Alban Bek, and Mehmet Emre Tasgin, “Engineering nonlinear response of nanomaterials using fano resonances,” *Journal of Optics* **16**, 105009 (2014).
 - ¹¹ Yizhuo Chu, Mohamad G Banaee, and Kenneth B Crozier, “Double-resonance plasmon substrates for surface-enhanced raman scattering with enhancement at excitation and stokes frequencies,” *Acs Nano* **4**, 2804–2810 (2010).
 - ¹² Niclas S. Mueller, Sebastian Heeg, and Stephanie Reich, “Surface-enhanced Raman scattering as a higher-order Raman process,” *Physical Review A* **94**, 1–13 (2016).
 - ¹³ Ado Jorio, Niclas S. Mueller, and Stephanie Reich, “Symmetry-derived selection rules for plasmon-enhanced Raman scattering,” *Physical Review B* **95**, 1–10 (2017).
 - ¹⁴ Boris Luk’yanchuk, Nikolay I Zheludev, Stefan A Maier, Naomi J Halas, Peter Nordlander, Harald Giessen, and Chong Tow Chong, “The fano resonance in plasmonic nanostructures and metamaterials,” *Nature materials* **9**, 707 (2010).
 - ¹⁵ Mikhail F Limonov, Mikhail V Rybin, Alexander N Poddubny, and Yuri S Kivshar, “Fano resonances in photonics,” *Nature Photonics* **11**, 543–554 (2017).
 - ¹⁶ Philippe Tassin, Lei Zhang, Th Koschny, EN Economou, and Costas M Soukoulis, “Low-loss metamaterials based on classical electromagnetically induced transparency,” *Physical Review Letters* **102**, 053901 (2009).
 - ¹⁷ Na Liu, Lutz Langguth, Thomas Weiss, Jürgen Kästel, Michael Fleischhauer, Tilman Pfau, and Harald Giessen, “Plasmonic analogue of electromagnetically induced transparency at the drude damping limit,” *Nature materials* **8**, 758 (2009).
 - ¹⁸ S M Sadeghi, W J Wing, and R R Gutha, “Undamped ultrafast pulsation of plasmonic fields via coherent exciton-plasmon coupling,” *Nanotechnology* **26**, 085202 (2015).
 - ¹⁹ Mehmet Emre Tasgin, “Metal nanoparticle plasmons operating within a quantum lifetime,” *Nanoscale* **5**, 8616–8624 (2013).
 - ²⁰ Mohamed ElKabbash, Alireza R. Rashed, Betul Kucukoz, Quang Nguyen, Ahmet Karatay, Gul Yaglioglu, Ekmele Ozbay, Humeyra Caglayan, and Giuseppe Strangi, “Ultrafast transient optical loss dynamics in excitonplasmon nano-assemblies,” *Nanoscale* **9**, 6558–6566 (2017).
 - ²¹ Bilge Can Yildiz Karakul, *Enhancement of plasmonic nonlinear conversion and polarization lifetime via fano resonances*, Ph.D. thesis, Middle East Technical University (2017).
 - ²² MA Noginov, G Zhu, AM Belgrave, Reuben Bakker, VM Shalaev, EE Narimanov, S Stout, E Herz, T Suteewong, and U Wiesner, “Demonstration of a spaser-based nanolaser,” *Nature* **460**, 1110 (2009).
 - ²³ Mark I. Stockman, “Nanoscience: Dark-hot resonances,” *Nature* **467**, 541–542 (2010).
 - ²⁴ Yu Zhang, Fangfang Wen, Yu-Rong Zhen, Peter Nordlander, and Naomi J. Halas, “Coherent Fano resonances in a plasmonic nanocluster enhance optical four-wave mixing,” *Proceedings of the National Academy of Sciences* **110**, 9215–9219 (2013).
 - ²⁵ Jian Ye, Fangfang Wen, Heidar Sobhani, J Britt Lassiter, Pol Van Dorpe, Peter Nordlander, and Naomi J Halas, “Plasmonic nanoclusters: near field properties of the fano resonance interrogated with sers,” *Nano letters* **12**, 1660–1667 (2012).
 - ²⁶ Yu Zhang, Yu-Rong Zhen, Oara Neumann, Jared K. Day, Peter Nordlander, and Naomi J. Halas, “Coherent anti-Stokes Raman scattering with single-molecule sensitivity using a plasmonic Fano resonance,” *Nature Communications* **5**, 1–7 (2014).
 - ²⁷ Mehmet Emre Tasgin, Ildar Salakhutdinov, Dania Kendziora, Musa Kurtulus Abak, Deniz Turkpence, Luca Piantanida, Ljiljana Fruk, Marco Lazzarino, and Alban Bek, “Fluorescence excitation by enhanced plasmon up-conversion under continuous wave illumination,” *Photonics and Nanostructures-Fundamentals and Applications* **21**, 32–43 (2016).
 - ²⁸ J Butet, G Bachelier, I Russier-Antoine, F Bertorelle, A Mosset, N Lascoux, C Jonin, E Benichou, and P-F Brevet, “Nonlinear fano profiles in the optical second-harmonic generation from silver nanoparticles,” *Physical Review B* **86**, 075430 (2012).
 - ²⁹ Alexander S Shorokhov, Elizaveta V Melik-Gaykazyan, Daria A Smirnova, Ben Hopkins, Katie E Chong, Duk-Yong Choi, Maxim R Shcherbakov, Andrey E Miroshnichenko, Dragomir N Neshev, Andrey A Fedyanin, *et al.*, “Multifold enhancement of third-harmonic generation in dielectric nanoparticles driven by magnetic fano resonances,” *Nano letters* **16**, 4857–4861 (2016).
 - ³⁰ Shailendra K Singh, M Kurtulus Abak, and Mehmet Emre Tasgin, “Enhancement of four-wave mixing via interference of multiple plasmonic conversion paths,” *Physical Review B* **93**, 035410 (2016).
 - ³¹ Emmanuel Paspalakis, Sofia Evangelou, Spyridon G Kossionis, and Andreas F Terzis, “Strongly modified four-wave mixing in a coupled semiconductor quantum dot-metal nanoparticle system,” *Journal of Applied Physics* **115**, 083106 (2014).
 - ³² R Zhang, Y Zhang, ZC Dong, S Jiang, C Zhang, LG Chen, L Zhang, Y Liao, J Aizpurua, Y ea Luo, *et al.*, “Chemical

- mapping of a single molecule by plasmon-enhanced raman scattering,” *Nature* **498**, 82 (2013).
- ³³ Janina Kneipp, Harald Kneipp, and Katrin Kneipp, “Sers—A single-molecule and nanoscale tool for bioanalytics,” *Chemical Society Reviews* **37**, 1052–1060 (2008).
- ³⁴ Ximei Qian, Xiang-Hong Peng, Dominic O Ansari, Qiqin Yin-Goen, Georgia Z Chen, Dong M Shin, Lily Yang, Andrew N Young, May D Wang, and Shuming Nie, “In vivo tumor targeting and spectroscopic detection with surface-enhanced raman nanoparticle tags,” *Nature biotechnology* **26**, 83–90 (2008).
- ³⁵ Yang Yang, John M Callahan, Tong-Ho Kim, April S Brown, and Henry O Everitt, “Ultraviolet nanoplasmonics: a demonstration of surface-enhanced raman spectroscopy, fluorescence, and photodegradation using gallium nanoparticles,” *Nano letters* **13**, 2837–2841 (2013).
- ³⁶ Chris B Schaffer, André Brodeur, and Eric Mazur, “Laser-induced breakdown and damage in bulk transparent materials induced by tightly focused femtosecond laser pulses,” *Measurement Science and Technology* **12**, 1784–1794 (2001).
- ³⁷ Taka-aki Yano, Yasushi Inouye, and Satoshi Kawata, “Nanoscale uniaxial pressure effect of a carbon nanotube bundle on tip-enhanced near-field raman spectra,” *Nano letters* **6**, 1269–1273 (2006).
- ³⁸ Wenqi Zhu and Kenneth B. Crozier, “Quantum mechanical limit to plasmonic enhancement as observed by surface-enhanced Raman scattering,” *Nature Communications* **5**, 5228 (2014).
- ³⁹ Kotni Santhosh, Ora Bitton, Lev Chuntonov, and Gilad Haran, “Vacuum rabi splitting in a plasmonic cavity at the single quantum emitter limit,” *Nature communications* **7**, ncomms11823 (2016).
- ⁴⁰ Mario Hentschel, Bernd Metzger, Bastian Knabe, Karsten Buse, and Harald Giessen, “Linear and nonlinear optical properties of hybrid metallic–dielectric plasmonic nanoantennas,” *Beilstein journal of nanotechnology* **7**, 111 (2016).
- ⁴¹ Gang L Liu, Yadong Yin, Siri Kunchakarra, Bipasha Mukherjee, Daniele Gerion, Stephen D Jett, David G Bear, Joe W Gray, A Paul Alivisatos, Luke P Lee, *et al.*, “A nanoplasmonic molecular ruler for measuring nuclease activity and dna footprinting,” *Nature nanotechnology* **1**, 47 (2006).
- ⁴² Steven J Barrow, Xingzhan Wei, Julia S Baldauf, Alison M Funston, and Paul Mulvaney, “The surface plasmon modes of self-assembled gold nanocrystals,” *Nature communications* **3**, 1275 (2012).
- ⁴³ See Supplemental Material at <http://...> for (i) (ii) (iii).
- ⁴⁴ Hui-Hsin Hsiao, Aimi Abass, Johannes Fischer, Rasoul Alaei, Andreas Wickberg, Martin Wegener, and Carsten Rockstuhl, “Enhancement of second-harmonic generation in nonlinear nanolaminate metamaterials by nanophotonic resonances,” *Optics express* **24**, 9651–9659 (2016).
- ⁴⁵ Krishnan Thyagarajan, Jeremy Butet, and Olivier JF Martin, “Augmenting second harmonic generation using fano resonances in plasmonic systems,” *Nano letters* **13**, 1847–1851 (2013).
- ⁴⁶ Ulrich Hohenester and Andreas Trügler, “Mnpbem—a matlab toolbox for the simulation of plasmonic nanoparticles,” *Computer Physics Communications* **183**, 370–381 (2012).
- ⁴⁷ Mikolaj K. Schmidt, Ruben Esteban, Alejandro González-Tudela, Geza Giedke, and Javier Aizpurua, “Quantum Mechanical Description of Raman Scattering from Molecules in Plasmonic Cavities,” *ACS Nano* **10**, 6291–6298 (2016), arXiv:1509.03851.
- ⁴⁸ Philippe Roelli, Christophe Galland, Nicolas Piro, and Tobias J. Kippenberg, “Molecular cavity optomechanics as a theory of plasmon-enhanced Raman scattering,” *Nature Nanotechnology* **11**, 164–169 (2015), arXiv:1407.1518.
- ⁴⁹ Malin Premaratne and Mark I Stockman, *Adv. Opt. Photon.*, Vol. 9 (2017) pp. 79–128.
- ⁵⁰ CL Garrido Alzar, MAG Martinez, and P Nussenzeig, “Classical analog of electromagnetically induced transparency,” *American Journal of Physics* **70**, 37–41 (2002).
- ⁵¹ Bumki Min, Eric Ostby, Volker Sorger, Erick Ulin-Avila, Lan Yang, Xiang Zhang, and Kerry Vahala, “High-Q surface-plasmon-polariton whispering-gallery microcavity,” *Natt. Lett.* **457** (2009).
- ⁵² Paul R West, Satoshi Ishii, Gururaj V Naik, Naresh K Emani, Vladimir M Shalaev, and Alexandra Boltasseva, “Searching for better plasmonic materials,” *Laser & Photonics Reviews* **4**, 795–808 (2010).
- ⁵³ Yih Horng Tan, Maozi Liu, Birte Nolting, Joan G Go, Jacquelyn Gervay-Hague, and Gang-yu Liu, “A nanoengineering approach for investigation and regulation of protein immobilization,” *ACS nano* **2**, 2374–2384 (2008).
- ⁵⁴ Sara D Costa, Cristiano Fantini, Ariete Righi, Alicja Bachmatiuk, Mark H Rummeli, Riichiro Saito, and Marcos A Pimenta, “Resonant raman spectroscopy on enriched ¹³C carbon nanotubes,” *Carbon* **49**, 4719–4723 (2011).
- ⁵⁵ Mehmet Emre Tasgin, Alpan Bek, and Selen Postaci, *Fano Resonances in Optics and Microwaves: Physics and Application* (Springer Review Book, to be published in 2018) Book Chapter 1: “Fano Resonances in the Linear and Nonlinear Plasmonic Response”.
- ⁵⁶ Johann Berthelot, Guillaume Bachelier, Mingxia Song, Padmnabh Rai, Gérard Colas Des Francs, Alain Dereux, and Alexandre Bouhelier, “Silencing and enhancement of second-harmonic generation in optical gap antennas,” *Optics express* **20**, 10498–10508 (2012).
- ⁵⁷ “Bem simulations,” http://physik.uni-graz.at/~uxh/mnpbem/html/mnpbem_ug_bemsimulations.html, accessed: 2017-09-22.